

# Impact on $|V_{us}|$ from $\tau$ decays: new *BABAR* results on $\tau^- \rightarrow K^- n \pi^0 \nu_\tau$ ( $n = 0, 1, 2, 3$ ) and $\tau^- \rightarrow \pi^- n \pi^0 \nu_\tau$ ( $n = 3, 4$ )

A. FILIPPI<sup>(1)</sup>ON BEHALF OF THE *BABAR* COLLABORATION<sup>(1)</sup> *I.N.F.N., Sezione di Torino - Torino, Italy*

**Summary.** — This paper reports preliminary measurements of the branching fractions of  $\tau$  hadronic decays in channels with one negative kaon or pion and multiple  $\pi^0$ 's:  $\tau^- \rightarrow K^- n \pi^0 \nu_\tau$  (with  $n = 0, 1, 2, 3$ ) and  $\tau^- \rightarrow \pi^- n \pi^0 \nu_\tau$  (with  $n = 3, 4$ ). These measurements are of fundamental importance for the precise determination of the  $|V_{us}|$  Cabibbo-Kobayashi-Maskawa matrix element. Based on a data sample of about 435 million  $\tau$  pairs produced in  $e^+e^-$  collisions at and near the  $\Upsilon(4S)$  peak, collected by the *BABAR* experiment in about ten years of data taking, the following values have been obtained:  $\mathcal{B}(\tau^- \rightarrow K^- \nu_\tau) = (7.174 \pm 0.033_{stat} \pm 0.213_{sys}) \times 10^{-3}$ ,  $\mathcal{B}(\tau^- \rightarrow K^- \pi^0 \nu_\tau) = (5.054 \pm 0.021_{stat} \pm 0.148_{sys}) \times 10^{-3}$ ,  $\mathcal{B}(\tau^- \rightarrow K^- 2\pi^0 \nu_\tau) = (6.151 \pm 0.117_{stat} \pm 0.338_{sys}) \times 10^{-4}$ ,  $\mathcal{B}(\tau^- \rightarrow K^- 3\pi^0 \nu_\tau) = (1.246 \pm 0.164_{stat} \pm 0.238_{sys}) \times 10^{-4}$ ,  $\mathcal{B}(\tau^- \rightarrow \pi^- 3\pi^0 \nu_\tau) = (1.168 \pm 0.006_{stat} \pm 0.038_{sys}) \times 10^{-2}$  and  $\mathcal{B}(\tau^- \rightarrow \pi^- 4\pi^0 \nu_\tau) = (9.020 \pm 0.400_{stat} \pm 0.652_{sys}) \times 10^{-4}$ .

14.40.Rt, 14.60.Fg

## 1. – Introduction

The measurement of  $\tau$  hadronic decays branching fractions in channels with strangeness provide a way to determine the value of the  $|V_{us}|$  Cabibbo-Kobayashi-Maskawa matrix element [1]. While extractions based on kaon semileptonic  $K_{\ell 3}$  and leptonic  $K_{\ell 2}$  decays agree with the values obtained applying unitarity relationships [1], the use of  $\tau$  lepton decay branching fractions provide values which are systematically lower and in tension, up to more than  $3\sigma$ , with the other derivations [1],[2]. To understand the origin of such a mismatch more precise measurements are desirable, especially for channels with neutral pions which are, so far, affected by the largest uncertainties. In fact, the experimental uncertainties of the decay branching ratios in channels with an odd number of kaons add up to the total uncertainty budget of  $|V_{us}|$  [2], as its determination accounts on the measurements of the inclusive branching ratio  $\mathcal{B}(\tau \rightarrow X_s \nu)$  and of the well-known  $\mathcal{B}(\tau \rightarrow \ell \nu_\ell \nu_\tau)$  semileptonic one [3].

The *BABAR* experiment [4], operating in the years 1999-2008 at the SLAC PEP-II  $e^+e^-$  machine, undertook a wide research program for the precise measurement of

the branching fractions of most of the hadronic  $\tau$  decay channels. About 435 million of  $\tau^+\tau^-$  pairs were used, from  $e^+e^-$  collisions at a center-of-mass energy of 10.58 GeV (and 40 MeV below), corresponding to an integrated luminosity of about  $500 \text{ fb}^{-1}$  with an average production cross-section  $\sigma(e^+e^- \rightarrow \tau^+\tau^-) = (0.919 \pm 0003) \text{ nb}$ . In this paper, preliminary results on the branching fractions of the decay channels  $\tau^- \rightarrow K^- n \pi^0 \nu_\tau$  ( $n = 0, 1, 2, 3$ ) and  $\tau^- \rightarrow \pi^- n \pi^0 \nu_\tau$  ( $n = 3, 4$ ) will be reported. Events with a possible presence of a  $K_S^0$  observed in its  $2\pi^0$  decay and of a  $\eta$  decaying in  $3\pi^0$  were discarded, so all decay channels proceeding through these particles were not included in the evaluation of the branching fractions.

## 2. – Data selection and analysis

The *BABAR* detector, described in detail elsewhere [4],[5], allowed for the full reconstruction of charged tracks by means of a five-layer silicon vertex detector and a 40-layer drift chamber, immersed inside a 1.5 T solenoidal magnetic field. Electron and photons could be identified by an electromagnetic calorimeter (EMC) composed by CsI(Tl) crystals. The hadron identification was provided by a ring-imaging Cherenkov detector (DIRC), which also delivered additional information for the lepton identification. The external magnetic field-flux return, which embedded the tracker, was instrumented with chambers for the detection of muons (IFR).

In order to identify  $\tau^- \rightarrow h^- n \pi^0 \nu_\tau$  events ( $h^- = K^-, \pi^-$ ), as well as their charge conjugate (wherever implied in this paper), events were selected with two oppositely charged tracks emitted in opposite hemispheres with respect to the event thrust axis in the reaction center of mass. The signal hemisphere contained the hadron, possible  $\pi^0$ 's and a neutrino; on the opposite side, one charged lepton from the  $\tau$  semileptonic decay tagged a  $\tau^+\tau^-$  event: so the typical signature for the searched reaction was two opposite prongs with some missing energy carried away by the unmeasured neutrinos. This jet-like topology is substantially different from that of a typical  $B\bar{B}$  event, for which the distribution of tracks is more isotropic and not just contained in opposite particle jets.

$\pi^0$ 's were reconstructed in the signal hemisphere by means of their  $\gamma\gamma$  decay: up to four  $\pi^0$ 's were allowed, while additional low energy photons, especially if emitted close to the charged signal track, were rejected. The  $\gamma\gamma$  system identified as  $\pi^0$  candidate was required to have an invariant mass of at least  $200 \text{ MeV}/c^2$ , with each  $\gamma$  opening angle with respect to the charged track smaller than 1.5 radians.

The oppositely charged tracks were required to be closer than 1.5 cm to the beam axis in the transverse plane, and closer than 2.5 cm to the interaction region along the beam axis; to allow for a good identification of the particles, the tracks needed to be well contained within the EMC and DIRC acceptance: in order to reach the DIRC, their transverse momentum was therefore required to be larger than  $250 \text{ MeV}/c$ . Tracks with a momentum larger than  $3.5 \text{ GeV}/c$  were rejected as well; this helped discarding the di-lepton background.

Several selection were applied in order to suppress background reactions.  $q\bar{q}$  events, as already mentioned, being characterized by an isotropic coverage of the detector fiducial volume, could be rejected by a selection on the event thrust, required to be less than 0.99, and on the event multiplicity.

Two photon events, with a typical emission of a fermion-antifermion pair in a  $e^+e^- \rightarrow \gamma^*\gamma^*e^+e^- \rightarrow e^+e^- f\bar{f}$  reaction could be rejected by applying a cut on the transverse momentum and missing energy. Bhabha and di-lepton events were moreover suppressed by a cut on the missing mass, taking into account that in the signal events there is an

energy unbalance due to three, overall, missing neutrinos. The missing mass is obtained subtracting the total four-momentum of the event from the center-of-mass four momentum, and was required to be larger than  $1 \text{ GeV}/c^2$  for events with reconstructed  $\pi^0$ 's, and larger than  $2.5 \text{ GeV}/c^2$  for events without them. To reject two-photon events the missing mass was required to be less than  $7.5 \text{ GeV}/c^2$ . If no  $\pi^0$  was reconstructed, a condition was additionally set on the ratio between the event transverse momentum  $p_T$  and the missing energy  $E_{miss} = \sqrt{s} - p_{tag} - p_{sig}$  (where  $p_{sig}$  and  $p_{tag}$  were, respectively, the moduli of the momenta of the detected hadron and the tagging lepton), requiring it to be larger than 0.2.

Events with  $K_L$  or other additional intermediate states were rejected imposing phase space conditions on the missing mass of tracks detected in the signal hemisphere, assuming that the decaying  $\tau$  gets half the energy available in the center of mass and its direction coincides with the event thrust vector.

The hadron and lepton identification is of paramount importance for the branching fraction measurement. To this end, the information provided by all the available detectors was exploited: kaons and pions could be identified thanks to the DIRC response, electrons, muons and hadrons could be distinguished by the shape of the showers induced on the EMC crystals, and the energy deposited by the track. Energy deposits in IFR could help separating muons and other hadrons. All tracks were subject to a sequential identification test (testing the identification hypotheses in the following order: muon, electron, kaon, pion), and the particle identification (PID) was assigned following the first successful response, if available, otherwise the track was not identified. Typical selection efficiencies for the reactions of interest ranged from 0.13%, for  $\tau^- \rightarrow K^- 3\pi^0 \nu_\tau$ , to 3.3% for  $\tau^- \rightarrow K^- \pi^0 \nu_\tau$ .

To improve the agreement between the particle identification efficiencies in real data and simulations, as compared to the standard figures of merit by *BABAR*, some custom procedures were developed. This is crucial since the extraction of the branching fraction heavily relies on simulated samples and their interplay, as will be explained in section 3. In particular, the  $\tau^- \rightarrow \pi^+ \pi^- \pi^- \nu_\tau$  and  $\tau^- \rightarrow K^+ K^- \pi^- \nu_\tau$  control samples were used to determine the efficiencies for the identification of true pions as pions, of true kaons as kaons and for the pion/kaon misidentification probability. Differently from the standard efficiencies derivation, the topology of these control samples is more similar to that of the reactions of interest, and the same rejection cuts can be applied. High purity samples of  $\pi$  and  $K$  were obtained from the mentioned reactions requiring the identification of two pions or of a  $K\pi$  pair, respectively. These pure samples were used to measure the PID efficiencies in different data taking periods, as a function of the particle charge and its kinematics (momentum and direction).

Also in the case of  $\pi^0$ 's some dedicated procedures were developed to improve the accuracy of identification efficiency in simulations. To this purpose, the reconstruction efficiencies were compared in experimental and simulated samples composed by a charged particle generically required not to be an electron and zero or one additional  $\pi^0$ 's, recoiling against an identified electron in the tagging hemisphere. In this way it was possible to extract a correction for the  $\pi^0$  efficiency to be applied to simulated data, which was dependent on the  $\pi^0$  momentum. On average, the correction weight turned out to be  $\eta_{\pi^0} = 0.958 \pm 0.01_{stat} \pm 0.009_{sys}$ , the statistical error being given by the sample size, while the systematic one depending on several sources among which the uncertainty on the  $\tau$  branching ratios values used in the simulation, on the amount of Bhabha events filtered in the control sample and on the split-off corrections which needed to be applied to compensate for an incorrect photon identification in EMC. This was indeed necessary as a

cluster of similar shape in the calorimeter crystals could be initiated by two overlapping photons or by a neutron, which could induce a split-off hadronic shower that could erroneously be associated to fake photons. The use of  $\tau^- \rightarrow \pi^- \nu_\tau$  and  $\tau^- \rightarrow \mu^- \bar{\nu}_\mu \nu_\tau$  decays as control samples allowed to determine the necessary correction factor. The simulated sample, in fact, describes fairly well the experimental data in the case of muons; on the other hand, in the pionic channel one can observe a mismatch in the distribution of distances of neutral clusters from the charged track, due to the incorrect identification on fake clusters at small distances (less than 40 cm), which determines an excess of data as compared to the simulated response (see Fig. 1). A correction factor  $\eta_{so} = 0.972$  was determined, to be applied to the simulated efficiency of extra photons in signal events with an identified pion or a kaon.

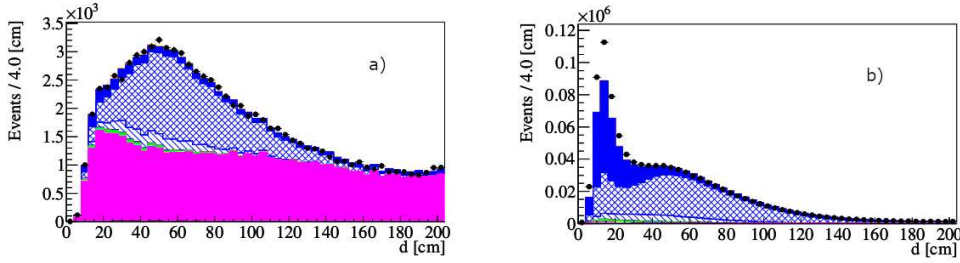


Fig. 1. – Distance between the intersection point of a track on EMC and the centroid of the closest photon cluster in the calorimeter. (a): distribution for  $\tau^- \rightarrow \mu^- \bar{\nu}_\mu \nu_\tau$  candidates, (b): distribution for  $\tau^- \rightarrow \pi^- \nu_\tau$  candidates. The contributions from simulated reactions (see legend of Fig. 2 for their list and corresponding patterns) are superimposed to the experimental points. From ref. [6].

### 3. – Branching fraction evaluation

The branching fraction for the  $\tau$  decay channel  $i$  is given by the following expression:

$$(1) \quad \mathcal{B}(\tau \rightarrow i) = 1 - \sqrt{1 - \frac{N_i^{prod}}{\mathcal{L}\sigma_{\tau\tau}}}$$

where  $\mathcal{L}$  is the integrated luminosity corresponding to the analyzed sample,  $\sigma_{\tau\tau}$  is the  $e^+e^- \rightarrow \tau^+\tau^-$  cross section at and around the  $\Upsilon(4S)$  peak [7, 8], and  $N_i^{prod}$  is the number of produced  $\tau$  pairs, efficiency corrected, for events with one of two signal candidates in the  $i$  decay channel. This number is obtained from the experimental observations taking however into account the fact that in each channel the selected candidates include not only signal events but also background contaminations from other decay modes (being signal modes or other kinds of decays), or from totally different reactions as mentioned above. The latter are rejected as much as possible by the mentioned selection cuts, and then their residual contributions are subtracted by means of Monte Carlo simulations of  $e^+e^-$  annihilations in  $\mu^+\mu^-$ ,  $\tau$  leptons or final states containing  $q\bar{q}$  light or heavy mesons ( $q = u, d, s, c, b$ ). The cross feeds from other signal modes, on the other hand, are determined by solving a system of linear equation through the migration matrix  $M_{ij}$ , which expresses the probability of reconstructing an event containing one or two  $i$  channel

decays into a different signal mode  $j$ :

$$(2) \quad N_i^{prod} = \sum_j (M^{-1})_{ij} (N_j^{sel} - N_j^{bck})$$

where  $N^{sel}$  and  $N^{bck}$  are the numbers of selected candidates and estimated background events, respectively.

The statistical errors on the signal yields are determined by the covariance matrix of the linear equation system, which propagates the independent statistical uncertainties of the number of candidates in each channel taking into account the cross-feeds between them.

The solution of the system of equations (2) delivers a set of numbers which indicate the relative contributions of each of the signal channels to a selected  $i$  decay mode. Pictorially, Fig. 2 shows the contribution to the momentum spectrum of the hadron ( $K^-$ ,  $\pi^-$ ) track of each of the considered signal channels: from it the cross-feed effect of different channels can be observed.

#### 4. – Systematic uncertainties evaluation

Several systematic effects must be taken into account in the extraction of the branching fractions; a summary of them and their contributions may be found in ref. [6] (see Tab. 1 and 3). The evaluation of their contribution to the final covariance matrix is based on varying for 50 times, according to a gaussian distribution with  $\sigma$  given by its statistical error, the value of each observable relevant for the branching fraction evaluation, and re-calculating the branching fractions starting from the modified value. All the uncertainties from independent sources are eventually summed up for the evaluation of the final systematic contribution.

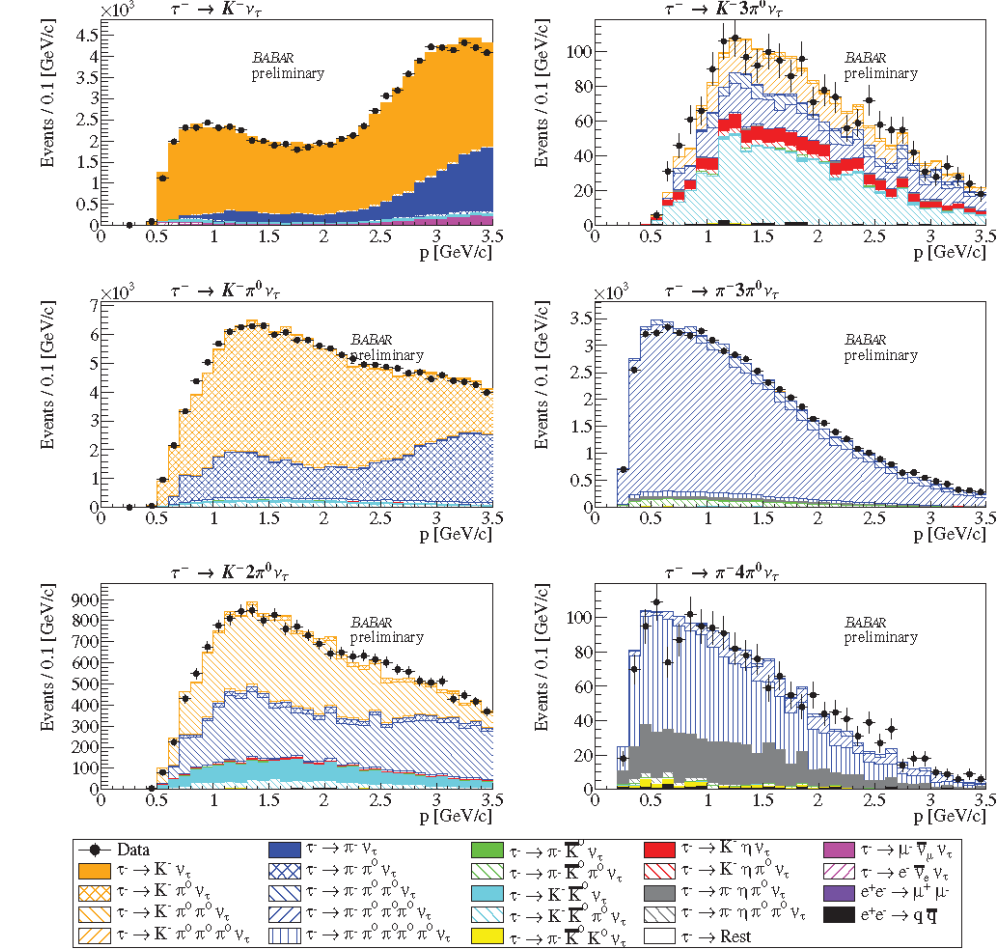
Some of the systematic uncertainties involve the detection efficiencies for signal and background decays, the particle identification efficiencies for charged particles and muons, and the tracking efficiency. The largest uncertainty affects the efficiency for  $\pi^0$  identification, and the mentioned corrections for its momentum dependence and the split-off effect. These uncertainties can be as large as 10%, especially in channels with several  $\pi^0$ 's. Other sources of systematic errors include, moreover, the uncertainty on the integrated luminosity, on the  $e^+e^- \rightarrow \tau^+\tau^-$  cross section and on the  $\tau$  decay branching fractions used for the simulation of the background channels.

The background simulations do not include the many-pion decays  $\tau^- \rightarrow \pi^- 5\pi^0 \nu_\tau$  and  $\tau^- \rightarrow K^- 4\pi^0 \nu_\tau$ : their omission brings therefore a systematic uncertainty which can be evaluated from the upper limit for the branching fractions of these channels. This upper limits, at 68% C.L., were determined using for selection efficiencies, as an approximation, those evaluated for the channels with one less pion, multiplied by the detection efficiency for a single, additional  $\pi^0$ .

#### 5. – Results

The following preliminary results for the  $\tau$  decay branching fractions in the channels under study have been obtained:

$$\mathcal{B}(\tau^- \rightarrow K^- \nu_\tau) = (7.174 \pm 0.033_{stat} \pm 0.213_{sys}) \times 10^{-3}$$



for channels with strangeness, as compared to the earlier measurements performed at LEP and Cornell [9]. The new result for  $\mathcal{B}(\tau^- \rightarrow K^- \nu_\tau)$  is consistent with an earlier result from BABAR [10], based, however, on a different tagging technique and obtained with an independent data sample. Another old result from BABAR [11], regarding  $\mathcal{B}(\tau^- \rightarrow K^- \pi^0 \nu_\tau)$ , must be updated by the new analysis, that exploits more refined methods especially for the treatment of systematic uncertainties, even though the two measurements partially share the same data set. The new and old measurement in this channel deviate from each other by  $3.8\sigma$ .

## 6. – Conclusions

With the new set of measurements, a large improvement on the precision of the  $|V_{us}|$  matrix element is expected, as a sizeable reduction of the uncertainties of most of the branching fractions for the  $\tau$  decay in hadronic channels with strangeness was pursued; most of the new results are the most precise measurements achieved so far. Including the new values in the averaging procedure, a reduction of the discrepancy of  $|V_{us}|$  to about  $3\sigma$  is preliminarily obtained [6], when comparing the derivation based on  $\tau \rightarrow s$ , kaon leptonic and semileptonic decays and CKM unitarity. This discrepancy still calls for new precise measurements in some other missing channels, to achieve a complete and exclusive description of the  $\tau$  hadronic decay modes.

## REFERENCES

- [1] HFLAV GROUP, AMHIS Y. *et al.*, *Eur. Phys. J. C*, **77** (2017) 9895.
- [2] LUSIANI A., *Proceedings of the 11<sup>th</sup> International Workshop on  $e^+e^-$  collisions from Phi to Psi (PhiPsi2017)*, Mainz, Germany, 2017, <https://inspirehep.net/record/1669594>, (2017) arXiv:1804.08436 [hep-ex].
- [3] GAMIZ E. *et al.*, *Jour. High Energy Phys.*, **01** (2003) 060;  
GAMIZ E. *et al.*, *Phys. Rev. Lett.*, **94** (2005) 011803.
- [4] BABAR COLLABORATION, AUBERT S. *et al.*, *Nucl. Inst. Methods A*, **479** (2002) 1.
- [5] BABAR COLLABORATION, AUBERT S. *et al.*, *Nucl. Inst. Methods A*, **729** (2013) 615.
- [6] LUSIANI A., *Proceedings of the 12<sup>th</sup> International Workshop on  $e^+e^-$  collisions from Phi to Psi (PhiPsi2019)*, BINP, Novosibirsk, Russia, 2019, *Eur. Phys. J. Web of Conferences*, **212** (2019) 08001.
- [7] JADACH S. *et al.*, *Comp. Phys. Comm.*, **130** (2000) 260.
- [8] BANERJEE S. *et al.*, *Phys. Rev. D*, **77** (2008) 054012.
- [9] PARTICLE DATA GROUP, PATRIGNANI C. *et al.*, *Chin. Phys. C*, **40** (2016) 100001.
- [10] BABAR COLLABORATION, AUBERT S. *et al.*, *Phys. Rev. Lett.*, **105** (2003) 051602.
- [11] BABAR COLLABORATION, LEES J.P. *et al.*, *Nucl. Inst. Methods A*, **726** (2013) 206.